Atmos. Chem. Phys. Discuss., 10, 9895–9916, 2010
www.atmos-chem-phys-discuss.net/10/9895/2010/

Atmospheric Chemistry and Physics Discussions

This discussion paper is/has been under review for the journal Atmospheric Chemistry and Physics (ACP). Please refer to the corresponding final paper in ACP if available.

Will climate change increase ozone depletion from low-energy-electron precipitation?

A. J. G. Baumgaertner[1], P. Jöckel[1,2], M. Dameris[2], and P. J. Crutzen[1]

[1]Max Planck Institute for Chemistry, 55020 Mainz, Germany
[2]Deutsches Zentrum für Luft-und Raumfahrt (DLR), Institut für Physik der Atmosphäre, Oberpfaffenhofen, 82234 Weßling, Germany

Received: 16 March 2010 – Accepted: 10 April 2010 – Published: 16 April 2010

Correspondence to: A. J. G. Baumgaertner (work@andreas-baumgaertner.net)

Published by Copernicus Publications on behalf of the European Geosciences Union.

Abstract

We investigate the effects of a strengthened Brewer-Dobson circulation on the transport of nitric oxide (NO) produced by energetic particle precipitation. During periods of high geomagnetic activity, low-energy-electron precipitation is responsible for winter time ozone loss in the polar middle atmosphere between 1 and 6 hPa. However, as climate change is expected to increase the strength of the Brewer-Dobson circulation, the enhancements of NO_x concentrations are expected to be transported to lower altitudes in extra-tropical regions, becoming even more significant in the ozone budget. We use simulations with the chemistry climate model system ECHAM5/MESSy to compare present day effects of low-energy-electron precipitation with expected effects in a climate change scenario for the year 2100. In years of strong geomagnetic activity, similar to that observed in 2003, an additional polar ozone loss of up to 0.5 µmol/mol at 5 hPa is found. However, this would be approximately compensated by an ozone enhancement originating from a stronger poleward transport of ozone from lower latitudes caused by a strengthened Brewer-Dobson circulation, as well as by slower photochemical ozone loss reactions in a stratosphere cooled by risen greenhouse gas concentrations.

1 Introduction

The Earth's middle and upper atmosphere are strongly influenced by solar variability. Changes in the solar spectral irradiance as well as in the solar wind can lead to significant perturbations. Solar wind disturbances have been shown to lead to geomagnetic activity variations, which can result in magnetospheric loss of electrons. These electrons precipitate into the atmosphere at high geomagnetic latitudes where they lead to the production of NO_x, termed EEP NO_x, through dissociation and ionisation processes. Downward transport in the dark polar winter can lead to significant enhancements of NO_x in the stratosphere. Because NO_x can catalytically destroy ozone, such NO_x enhancements lead to ozone depletion in the upper stratosphere as has

ACPD

10, 9895–9916, 2010

been shown e.g. by Callis et al. (1998); Brasseur and Solomon (2005); Jackman et al. (2008); Baumgaertner et al. (2009). In the mesosphere and lower thermosphere (MLT), the mean meridional circulation transports air from the summer to the winter hemisphere, driven by radiative heating and cooling, respectively (Brasseur and Solomon, 2005). In the polar winter, this circulation can transport air, including EEP induced NO_x enhancements, from the MLT into the stratosphere. In the polar stratosphere, further downward transport is controlled by the Brewer-Dobson (B-D) circulation. The B-D circulation is responsible for the meridional transport of air in the stratosphere: It mainly consists of poleward transport in the middle and upper stratosphere, with rising air in the tropics and downwelling in the polar regions. Model studies have reported that climate change leads to a strengthening of the B-D circulation. One of the first model predictions of this strengthening was published by Butchart and Scaife (2001), who already attributed their findings to changes in planetary wave driving. Further studies of this phenomenon were conducted by e.g. Butchart et al. (2006); Butchart et al. (2010); Deckert and Dameris (2008); McLandress and Shepherd (2009); Garny et al. (2009). To date, a full picture of the mechanisms that strengthen the B-D circulation has not yet been established. However, there is some evidence for an opening of the subtropical jets due to greenhouse warming, leading to changes in the transient Rossby wave drag (T. Shepherd, personal communication, 2009).

A stronger meridional circulation would also lead to stronger downwelling in the stratosphere in polar winter, transporting EEP NO_x to lower altitudes than before. Since ozone concentrations maximise in the lower stratosphere, the lower NO_x is transported the more important it can potentially become in the ozone budget.

Here, we investigate the impact of a strengthened B-D circulation on polar stratospheric ozone using the ECHAM5/MESSy Atmospheric Chemistry (EMAC) climate model EMAC. The climate change scenario SRES A2 (Nakicenovic et al., 2000) is used for the year 2100 in order to drive simulations with a stronger B-D circulation. All simulations for present day and year-2100 conditions have repeating boundary conditions, meaning that sea surface temperatures (SST), emissions, etc. were repeated

on a yearly basis to minimise inter-annual variability induced by these boundary conditions. Four simulations are needed to extract the desired signal: Two simulations were performed for the year 2100, where the EEP NO_x source was switched on in the first simulation and switched off in the second. Another two simulations were carried out for present day conditions, again with EEP NO_x on and off, respectively. The model and the model setup are described in Sect. 2, the results are discussed in Sect. 3, and conclusions are presented in Sect. 4.

2 Model description, configuration, and setup

2.1 The model EMAC

The ECHAM/MESSy Atmospheric Chemistry model is a numerical chemistry and climate simulation system that includes sub-models describing tropospheric and middle atmosphere processes and their interaction with oceans, land and human influences (Jöckel et al., 2006). It uses the Modular Earth Submodel System (MESSy) to link multi-institutional computer codes. The core atmospheric model is the 5th generation European Centre Hamburg general circulation model (ECHAM5, Roeckner et al., 2006). The model has been shown to consistently simulate key atmospheric tracers such as ozone (Jöckel et al., 2006), water vapour (Lelieveld et al., 2007), and lower and middle stratospheric NO_y (Brühl et al., 2007). For the present study we applied EMAC (ECHAM5 version 5.3.02, MESSy version 1.8+) in the T42L90MA-resolution, i.e. with a spherical triangular truncation of T42 (corresponding to a quadratic Gaussian grid of approximately 2.8° by 2.8° in latitude and longitude) with 90 vertical hybrid pressure levels up to 0.01 hPa.

The following MESSy submodels were used: CLOUD (cloud routines), CONVECT (convection parametrisation, see Tost et al., 2006b), CVTRANS (convective tracer transport), DRYDEP (dry deposition, see Kerkweg et al., 2006a), H2O (consistent feedback of the chemical tracer water vapour with specific humidity of the base model),

ACPD
10, 9895–9916, 2010

JVAL (based on Landgraf and Crutzen, 1998), LNOX (a lightning NO_x parametrisation, see Tost et al., 2007), MECCA (Sander et al., 2005), PSC (polar stratospheric clouds), OFFLEM and ONLEM (offline emission and online calculated emission of trace gases, see Kerkweg et al., 2006b), RAD4ALL (radiation code), SCAV (scavenging parametrisation by Tost et al., 2006a), SEDI, SPACENOX (Baumgaertner et al., 2009), TNUDGE (Newtonian relaxation of long-lived trace gases at the surface, see Kerkweg et al., 2006b), TROPOP (diagnostics submodel).

The chosen chemistry scheme for the configuration of the submodel MECCA is simpler compared to the configuration in Jöckel et al. (2006). For example, the NMHC (non-methane hydrocarbon) chemistry is not treated at the same level of detail. The complete mechanism is documented in the supplement at http://www.atmos-chem-phys-discuss.net/10/9895/2010/acpd-10-9895-2010-supplement.pdf.

2.2 Model setup for present day simulations

Simulations were performed for present day and for year-2100 conditions. The concentrations of long-lived trace gases (CO_2, CH_4, N_2O, and SF_6, as well as Chlorine and Bromine containing substances) are relaxed to prescribed present day values at the surface. Finally, present day emissions of short-lived trace gases from the surface, the boundary layer, and aircraft (NO_x, NMHCs, CO, SO_2, NH_3) were applied similar to Jöckel et al. (2006). The present-day simulations use the AMIPIIb sea ice and sea surface temperature (SST) data set. The El Niño-Southern Oscillation (ENSO) can lead to large-scale deviations of tropical SSTs from the long-term mean (see e.g. Harrison and Larkin, 1998; Enfield, 1989). During the El Niño phase, SSTs in the tropical pacific rise by more than two Kelvin, during La Niña events this area is colder than normal. Therefore, we used climatological SSTs from AMIPIIb where neither El Niño nor La Niña events occur. Figure 1 shows the anomalies of the employed SSTs for December with respect to the long-term December mean (1980–2000). Temperature anomalies are below 0.5 K throughout the tropical Pacific, and the SSTs are therefore not biased by an El Niño or La Niña event.

2.3 Model setup for year-2100 simulations

For the simulations with year-2100 conditions in a climate change scenario, the SRES A2 scenario (IPCC Special Report on Emissions Scenarios, Nakicenovic et al., 2000) was chosen, which describes an economic development which is primarily regionally oriented and the technical change is more fragmented and slower than in the other SRES storylines. In terms of climate-change induced surface temperature increase it is the most drastic, resulting in an increase of approx. 4 K depending on the model (IPCC, 2007). We expect that this scenario also causes the strongest B-D circulation enhancement, so that effects on EEP NO_x and polar ozone can be clearly distinguished from other sources of variability.

SSTs and sea ice coverage as well as the concentrations of greenhouse gases are the most important boundary conditions that are required to simulate a future climate. SST and sea ice coverage data were taken from an IPCC AR4 simulation including an interactive ocean model, ECHAM5/MPIOM, see Jungclaus (2006).

Analogously to the year 2000, we show that the employed SSTs are not biased by El Niño or La Niña events. Figure 2 shows the anomalies of the employed SSTs for December 2099 with respect to the December mean from 2080–2099. In the tropical pacific, anomalies are generally smaller than 1.5 K and do not show the typical El Niño or La Niña pattern.

Figure 3 depicts the mean difference between the SSTs from the year 2099 as predicted by ECHAM5/MPIOM, and present day (taken from AMIPIIb, see above). Most areas show a marked increase of several Kelvin as expected.

For CO_2, CH_4, and N_2O the initial concentrations as well as the prescribed database of surface concentrations were scaled to the expected concentrations of the trace gases in the year 2100 (SRES A2 scenario), using the information provided in Nakicenovic et al. (2000) and IPCC (2007). This yields mean surface mixing ratios of 850 µmol/mol for CO_2, 3400 nmol/mol for CH_4, and 450 nmol/mol for N_2O.

ACPD
10, 9895–9916, 2010

2.3.1 Solar and geomagnetic variability

The model contains most mechanisms of solar variability that are known to influence the lower and middle atmosphere. This includes effects from solar shortwave flux variability on radiative heating and photolysis, NO_x formation by Galactic Cosmic Rays, HO_X and NO_x production by Solar Proton Events, and NO_x production in the MLT through energetic electron precipitation (EEP). As discussed in Sect. 1, the latter process can lead to NO_x enhancements (EEP NO_x) that are transported down into the stratosphere. The model implementation of this process is described by Baumgaertner et al. (2009).

In order to explicitly eliminate the influence of variability in the solar shortwave flux and SSTs, the shortwave flux was kept constant and SSTs were repeated on a 12-month basis. Solar Proton Events were not included in the model simulations because of their sporadic occurrence. The EEP strength for production of NO_x in the mesosphere and lower thermosphere was set to 2003 with repeating monthly A_p values as input, shown in Fig. 4. The A_p index is a commonly used measure of global geomagnetic activity and is derived from magnetic field component measurements at 13 subauroral geomagnetic observatories (Mayaud, 1980). In particular the Southern Hemisphere winter 2003 experienced strong enhancements of EEP NO_x (Funke et al., 2005; Randall et al., 2007). This large perturbation will make it possible to identify the effects focused on in this study most clearly.

3 Results

In order to evaluate the effects of climate change, more specifically a changed B-D circulation, on the extent and the properties of EEP NO_x enhancements, several simulations have to be performed and compared. We cannot simply compare two simulations, one for present day conditions and one for the year 2100, to analyse these effects. This is because in the simulation for the year-2100 climate change has affected the mean state of the atmosphere such that the induced EEP NO_x changes are difficult

ACPD
10, 9895–9916, 2010

to distinguish from other changes in the NO_x and ozone distributions. Therefore, four simulations were carried out:

Simulation S-PRESENT-EEP. Model setup as described in Sect. 2.2. The EEP NO_x source submodel was turned on.

Simulation S-PRESENT. As S-PRESENT-EEP but with the EEP NO_x source submodel turned off.

Simulation S-Y2100-EEP. Model setup as described in Sect. 2.3 for year 2100 conditions. The EEP NO_x source submodel was turned on.

Simulation S-Y2100. As S-Y2100-EEP but with the EEP NO_x source submodel turned off.

The simulations S-PRESENT and S-Y2100 were integrated for a spin-up period of three years. The resulting model state was used as the starting point for the four simulations described above. Each of these simulations was performed for nine model years.

To obtain the climate-change induced EEP NO_x changes the following procedure is adopted. These steps are independent of the quantity of interest, i.e. NO_x or ozone. In a first step the basic EEP related changes are calculated separately for both year-2100 conditions and present conditions. Then, the result obtained for present day is subtracted from the year-2100 result, yielding only the changes in EEP effects due to climate change. A diagram of this procedure is presented in Fig. 5.

Since the model setup similar to the one used here has been evaluated extensively in several studies (Jöckel et al., 2006; Lelieveld et al., 2007; Brühl et al., 2007; Baumgaertner et al., 2009), we do not present an evaluation of the model. However, an evaluation of the model with respect to the changes made for the year-2100 simulations is necessary. In order to check if the year-2100 simulations experience a stronger B-D circulation, we analyse the changes in the mean ozone distribution. Figure 6 shows the change in the annual zonal mean ozone mixing ratios between simulations S-PRESENT and S-Y2100. A decrease of up to 0.4 µmol/mol is found in the tropical and subtropical lower stratosphere, at higher latitudes an increase of the same amount

ACPD
10, 9895–9916, 2010

reaches down to 40 hPa. These changes are consistent with a strengthening of the B-D circulation and similar changes have been reported by Li et al. (2009), see their Fig. 2, who compared differences between 2060–2069 and 1975–1984. In the upper stratosphere ozone increased by up to 1.6 µmol/mol, also similar to the results from Li et al. (2009). This is due to the increase of greenhouse gas concentrations which leads to a cooling of the stratosphere (not shown), which in turn slows down the temperature dependent photochemical ozone loss reactions (e.g. Barnett et al., 1975; Haigh and Pyle, 1982).

Having shown indications for the expected strengthening of the B-D circulation, we now analyse changes in NO_x and ozone using the four simulations and the processing technique described above. The zonal mean NO_x changes for the July–September mean, i.e. Southern Hemisphere winter/spring, averaged over all years are shown in Fig. 7. A paired t-test of the null hypothesis that data in the difference (year-2100)–(present day) are a random sample from a normal distribution with mean 0 was performed. Areas, where the test fails at the 1% significance level, i.e. where the changes are statistically significant, are shaded. It is evident, that the enhanced B-D circulation leads to a significant enhancement of 5 nmol/mol EEP NO_x in the polar upper stratosphere.

Similarly, Fig. 8 shows the associated changes in ozone. NO_x enhancements between 1 and 8 hPa south of 60° S are mirrored by a decrease in ozone of up to 0.5 µmol/mol in areas where sunlight and thus atomic oxygen is present which allows the catalytic destruction of ozone to proceed. The t-test at the 1% significance levels, indicated as the shaded areas, shows that the decrease is significant at least in half of the area.

From Fig. 6 we found that the employed climate change scenario leads to an increase of ozone mixing ratios of up to 0.8 µmol/mol in the upper stratosphere south of 60° S in the mean, for the period July–September only this increase is as large as 1.1 µmol/mol (not shown). Two processes related to climate change lead to this effect. Firstly, a strengthened B-D circulation also transports more low- and mid-latitude ozone to the

polar area. Secondly, cooling of the stratosphere due to enhanced greenhouse gas concentrations leads to slower photochemical ozone loss reactions, globally enhancing ozone mixing ratios in the upper stratosphere. As a net result, these two processes approximately compensate the loss of ozone associated with stronger downward transport of EEP NO_x.

4 Conclusions

Climate change leads to a stronger B-D circulation in the presented ECHAM5/MESSy simulations. Associated stronger downward transport of EEP NO_x in the polar winter stratosphere leads to an additional 3–5 nmol/mol of NO_x between 2 and 8 hPa under year-2100 conditions. This, in turn, causes some additional ozone loss up to 0.5 µmol/mol in this area. However, the ozone loss is approximately compensated for by an enhanced transport of ozone from low- and mid-latitudes as well as a slower photochemical ozone loss reaction.

Development of a whole atmosphere model is underway; this will include the middle and upper atmosphere model CMAT2 (UCL London, see e.g Yiğit et al., 2009) into MESSy allowing for a better representation of upper atmospheric NO_x and thus make is possible to much more accurately study EEP NO_x transport and effects.

Acknowledgements. We thank all MESSy developers for their contributions and help. This research was funded by the TIES project within the DFG SPP 1176 CAWSES. The Ferret program (http://www.ferret.noaa.gov) from NOAA's Pacific Marine Environmental Laboratory was used for creating some of the graphics in this paper. The model simulations were performed on the POWER-6 computer at the DKRZ.

The service charges for this open access publication have been covered by the Max Planck Society.

References

Barnett, J. J., Houghton, J. T., and Pyle, J. A.: The temperature dependence of the ozone concentration near the stratopause, Q. J. Roy. Meteor. Soc., 101, 245–257, doi:10.1002/qj.49710142808, 1975. 9903

Baumgaertner, A. J. G., Jöckel, P., and Brühl, C.: Energetic particle precipitation in ECHAM5/MESSy1 – Part 1: Downward transport of upper atmospheric NO_x produced by low-energy-electrons, Atmos. Chem. Phys., 9, 2729–2740, 2009, http://www.atmos-chem-phys.net/9/2729/2009/. 9897, 9899, 9901, 9902

Baumgaertner, A. J. G., Jöckel, P., Riede, H., Stiller, G., and Funke, B.: Energetic particle precipitation in ECHAM5/MESSy – Part 2: Solar Proton Events, Atmos. Chem. Phys. Discuss., 10, 4501–4542, 2010, http://www.atmos-chem-phys-discuss.net/10/4501/2010/.

Brasseur, G. P. and Solomon, S.: Aeronomy of the Middle Atmosphere: Chemistry and Physics of the Stratosphere and Mesosphere, Springer, third edn., 2005. 9897

Brühl, C., Steil, B., Stiller, G., Funke, B., and Jöckel, P.: Nitrogen compounds and ozone in the stratosphere: comparison of MIPAS satellite data with the chemistry climate model ECHAM5/MESSy1, Atmos. Chem. Phys., 7, 5585–5598, 2007, http://www.atmos-chem-phys.net/7/5585/2007/. 9898, 9902

Butchart, N. and Scaife, A. A.: Removal of chlorofluorocarbons by increased mass exchange between the stratosphere and troposphere in a changing climate, Nature, 410, 799–802, 2001. 9897

Butchart, N., Scaife, A. A., Bourqui, M., de Grandpré, J., Hare, S. H. E., Kettleborough, J., Langematz, U., Manzini, E., Sassi, F., Shibata, K., Shindell, D., and Sigmond, M.: Simulations of anthropogenic change in the strength of the Brewer Dobson circulation, Clim. Dynam., 27, 727–741, doi:10.1007/s00382-006-0162-4, 2006. 9897

Butchart, N., Cionni, I., Eyring, V., Shepherd, T. G., Waugh, D. W., Akiyoshi, H., Austin, J., Brühl, C., Chipperfield, M. P., Cordero, E., Dameris, M., Deckert, R., Dhomse, S., Frith, S. M., Garcia, R. R., Gettelman, A., Giorgetta, M. A., Kinnison, D. E., Li, F., Mancini, E., McLandress, C., Pawson, S., Pitari, G., Plummer, D. A., Rozanov, E., Sassi, F., Scinocca, J. F., Shibata, K., Steil, B., and Tian, W.: Chemistry-climate model simulations of 21st century stratospheric climate and circulation changes, J. Climate, accepted, 2010. 9897

Callis, L. B., Natarajan, M., Lambeth, J. D., and Baker, D. N.: Solar – atmospheric coupling

by electrons (SOLACE). 2. Calculated stratospheric effects of precipitating electrons, 1979-1988., J. Geophys. Res., 103, 28421–28438, doi:10.1029/98JD02407, 1998. 9897
Deckert, R. and Dameris, M.: Higher tropical SSTs strengthen the tropical upwelling via deep convection, Geophys. Res. Lett., 35, L10813, doi:10.1029/2008GL033719, 2008. 9897
Enfield, D. B.: El Nino, past and present, Rev. Geophys., 27, 159–187, doi:10.1029/RG027i001p00159, 1989. 9899
Funke, B., López-Puertas, M., Gil-López, S., von Clarmann, T., Stiller, G. P., Fischer, H., and Kellmann, S.: Downward transport of upper atmospheric NO_x into the polar stratosphere and lower mesosphere during the Antarctic 2003 and Arctic 2002/2003 winters, J. Geophys. Res., 110, D24308, doi:10.1029/2005JD006463, 2005. 9901
Garny, H., Dameris, M., and Stenke, A.: Impact of prescribed SSTs on climatologies and long-term trends in CCM simulations, Atmos. Chem. Phys., 9, 6017–6031, 2009, http://www.atmos-chem-phys.net/9/6017/2009/. 9897
Haigh, J. D. and Pyle, J. A.: Ozone perturbation experiments in a two-dimensional circulation model, Q. J. Roy. Meteor. Soc., 108, 551–574, doi:10.1256/smsqj.45704, 1982. 9903
Harrison, D. E. and Larkin, N. K.: El Niño-Southern Oscillation sea surface temperature and wind anomalies, 1946-1993, Rev. Geophys., 36, 353–400, doi:10.1029/98RG00715, 1998. 9899
IPCC: IPCC Fourth Assessment Report: Climate Change 2007, Cambridge University Press, Cambridge, 2007. 9900
Jackman, C. H., Marsh, D. R., Vitt, F. M., Garcia, R. R., Fleming, E. L., Labow, G. J., Randall, C. E., Lpez-Puertas, M., Funke, B., von Clarmann, T., and Stiller, G. P.: Short- and medium-term atmospheric constituent effects of very large solar proton events, Atmos. Chem. Phys., 8, 765–785, 2008, http://www.atmos-chem-phys.net/8/765/2008/. 9897
Jöckel, P., Tost, H., Pozzer, A., Brühl, C., Buchholz, J., Ganzeveld, L., Hoor, P., Kerkweg, A., Lawrence, M. G., Sander, R., Steil, B., Stiller, G., Tanarhte, M., Taraborrelli, D., van Aardenne, J., and Lelieveld, J.: The atmospheric chemistry general circulation model ECHAM5/MESSy1: consistent simulation of ozone from the surface to the mesosphere, Atmos. Chem. Phys., 6, 5067–5104, 2006, http://www.atmos-chem-phys.net/6/5067/2006/. 9898, 9899, 9902
Jungclaus, J.: IPCC-AR4 MPI-ECHAM5_T63L31 MPI-OM_GR1.5L40 SRESA2 run no.3: ocean monthly mean values MPImet/MaD Germany. World Data Center for Climate. CERA-DB

”OM-GR1.5L40_EH5-T63L31_A2_3_MM”, 2006. 9900, 9910, 9911
Kerkweg, A., Buchholz, J., Ganzeveld, L., Pozzer, A., Tost, H., and Jöckel, P.: Technical Note: An implementation of the dry removal processes DRY DEPosition and SEDImentation in the Modular Earth Submodel System (MESSy), Atmos. Chem. Phys., 6, 4617–4632, 2006a, http://www.atmos-chem-phys.net/6/4617/2006/. 9898
Kerkweg, A., Sander, R., Tost, H., and Jöckel, P.: Technical note: Implementation of prescribed (OFFLEM), calculated (ONLEM), and pseudo-emissions (TNUDGE) of chemical species in the Modular Earth Submodel System (MESSy), Atmos. Chem. Phys., 6, 3603–3609, 2006b, http://www.atmos-chem-phys.net/6/3603/2006/. 9899
Landgraf, J. and Crutzen, P. J.: An Efficient Method for Online Calculations of Photolysis and Heating Rates., J. Atmos. Sci., 55, 863–878, doi:10.1175/1520-0469(1998)055, 1998. 9899
Lelieveld, J., Brühl, C., Jöckel, P., Steil, B., Crutzen, P. J., Fischer, H., Giorgetta, M. A., Hoor, P., Lawrence, M. G., Sausen, R., and Tost, H.: Stratospheric dryness: model simulations and satellite observations, Atmos. Chem. Phys., 7, 1313–1332, 2007, http://www.atmos-chem-phys.net/7/1313/2007/. 9898, 9902
Li, F., Stolarski, R. S., and Newman, P. A.: Stratospheric ozone in the post-CFC era, Atmos. Chem. Phys., 9, 2207–2213, 2009, http://www.atmos-chem-phys.net/9/2207/2009/. 9903
Mayaud, P. N.: Derivation, Meaning, and Use of Geomagnetic Indices, Geophysical Monograph 22, Am. Geophys. Union, Washington D.C., 1980. 9901
McLandress, C. and Shepherd, T. G.: Simulated Anthropogenic Changes in the Brewer–Dobson Circulation, Including Its Extension to High Latitudes, J. Climate, 22, 1516–1540, doi:10.1175/2008JCLI2679.1, 2009. 9897
Nakicenovic, N., Alcamo, J., Davis, G., de Vries, B., Fenhann, B., Gaffin, S., Gregory K., Grübler, A., Jung, T. Y., Kram, T., La Rovere, E. L., Michaelis, E. L., Mori, S., Morita, T., Pepper, W., Pitcher, H., Price, L., Raihi, K., Roehrl, A., Rogner, H.-H., Sankovski, A., Schlesinger, M., Shukla, P., Smith, S., Swart, R., van Rooijen, S., Victor, N., and Dadi, Z.: IPCC Special Report on Emissions Scenarios, Cambridge University Press, UK and New York, NY, USA, 2000. 9897, 9900
Randall, C. E., Harvey, V. L., Singleton, C. S., Bailey, S. M., Bernath, P. F., Codrescu, M., Nakajima, H., and Russell, J. M.: Energetic particle precipitation effects on the Southern Hemisphere stratosphere in 1992-2005, J. Geophys. Res., 112, D08308, doi:10.1029/2006JD007696, 2007. 9901

ACPD
10, 9895–9916, 2010

Roeckner, E., Brokopf, R., Esch, M., Giorgetta, M., Hagemann, S., Kornblueh, L., Manzini, E., Schlese, U., and Schulzweida, U.: Sensitivity of Simulated Climate to Horizontal and Vertical Resolution in the ECHAM5 Atmosphere Model, J. Climate, 19, 3771, doi:10.1175/JCLI3824.1, 2006. 9898

Sander, R., Kerkweg, A., Jöckel, P., and Lelieveld, J.: Technical note: The new comprehensive atmospheric chemistry module MECCA, Atmos. Chem. Phys., 5, 445–450, 2005, http://www.atmos-chem-phys.net/5/445/2005/. 9899

Tost, H., Jckel, P., Kerkweg, A., Sander, R., and Lelieveld, J.: Technical note: A new comprehensive SCAVenging submodel for global atmospheric chemistry modelling, Atmos. Chem. Phys., 6, 565–574, 2006a, http://www.atmos-chem-phys.net/6/565/2006/. 9899

Tost, H., Jöckel, P., and Lelieveld, J.: Influence of different convection parameterisations in a GCM, Atmos. Chem. Phys., 6, 5475–5493, 2006b, http://www.atmos-chem-phys.net/6/5475/2006/. 9898

Tost, H., Jöckel, P., and Lelieveld, J.: Lightning and convection parameterisations uncertainties in global modelling, Atmos. Chem. Phys., 7, 4553–4568, 2007, http://www.atmos-chem-phys.net/7/4553/2007/. 9899

Yiğit, E., Medvedev, A. S., Aylward, A. D., Hartogh, P., and Harris, M. J.: Modeling the effects of gravity wave momentum deposition on the general circulation above the turbopause, J. Geophys. Res., 114, D07101, doi:10.1029/2008JD011132, 2009. 9904

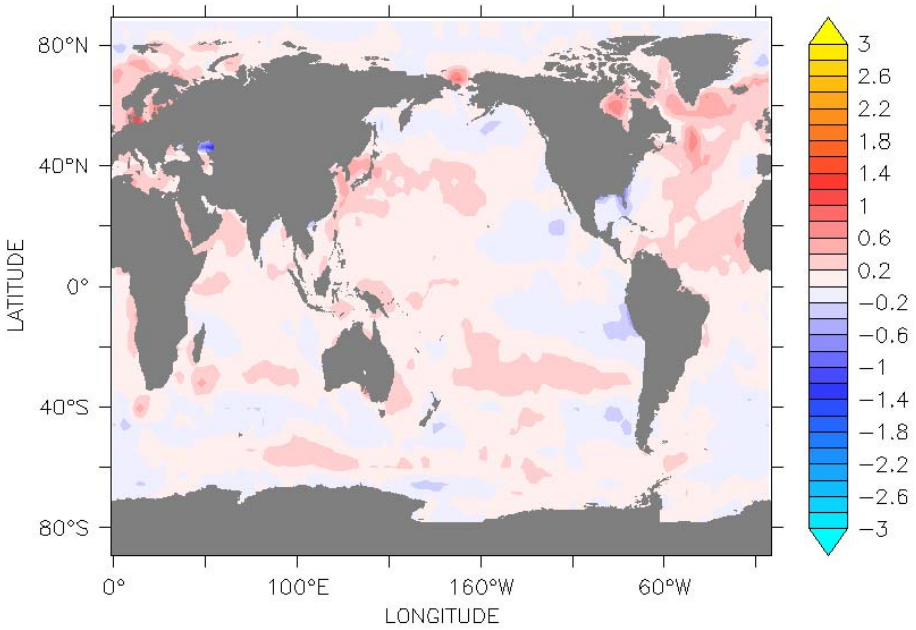

Fig. 1. Present-day sea surface temperature (AMIPIIb) anomalies for December with respect to the long-term mean (2080–2099).

ACPD
10, 9895–9916, 2010

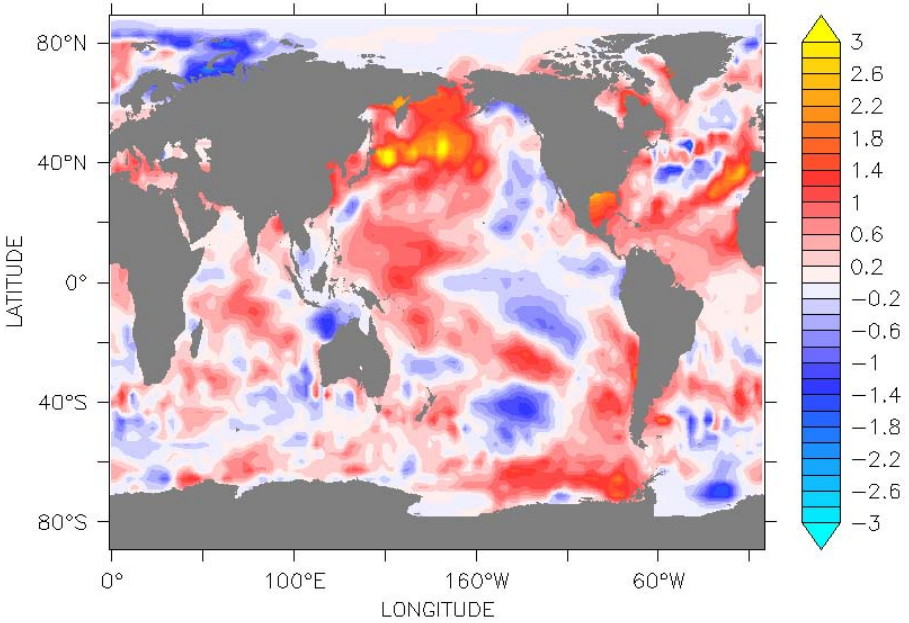

Fig. 2. Sea surface temperature (IPCC AR4 model simulation, see Jungclaus, 2006) anomalies for December 2100 with respect to the long-term mean (1980–2000).

ACPD
10, 9895–9916, 2010

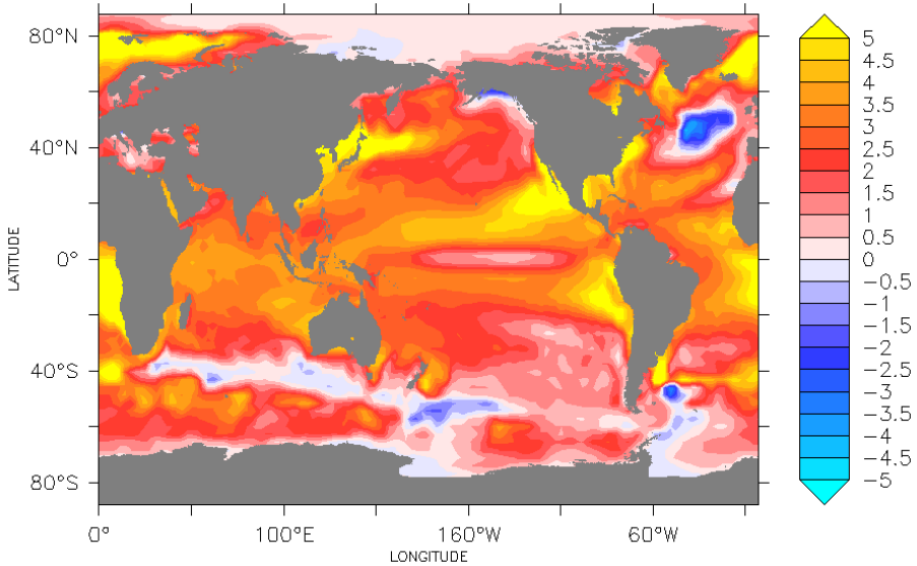

Fig. 3. Sea surface temperature difference between present day (year 2000 from HadISST1) and year 2100 (IPCC AR4 model simulation, Jungclaus (2006).

ACPD
10, 9895–9916, 2010

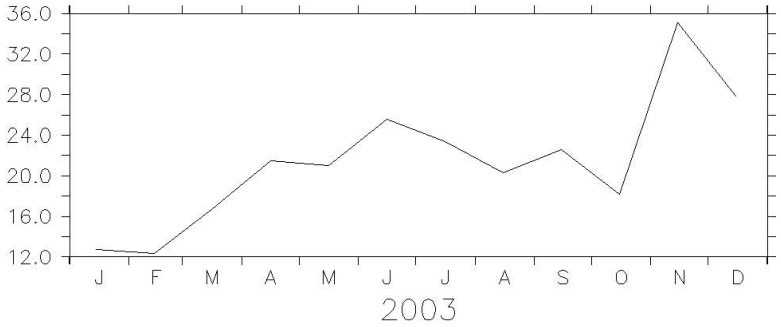

Fig. 4. Monthly average A_p index for the year 2003 which is used as input for the EEP parametrisation.

ACPD
10, 9895–9916, 2010

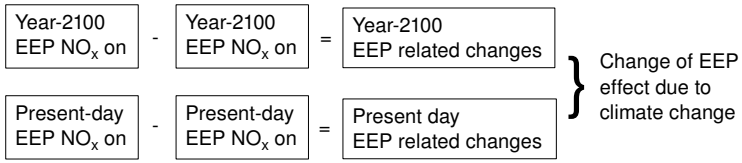

Fig. 5. Overview of the performed simulations and the performed processing.

ACPD
10, 9895–9916, 2010

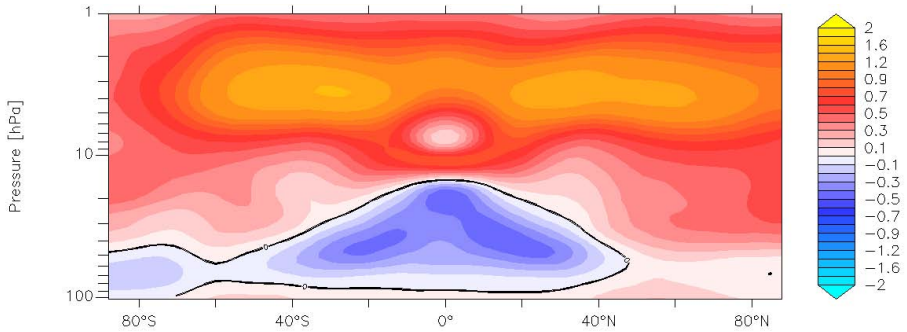

Fig. 6. Change of annual zonal mean ozone mixing ratios (µmol/mol) in the year 2100 (S-Y2100) with respect to present day conditions (S-PRESENT).

ACPD
10, 9895–9916, 2010

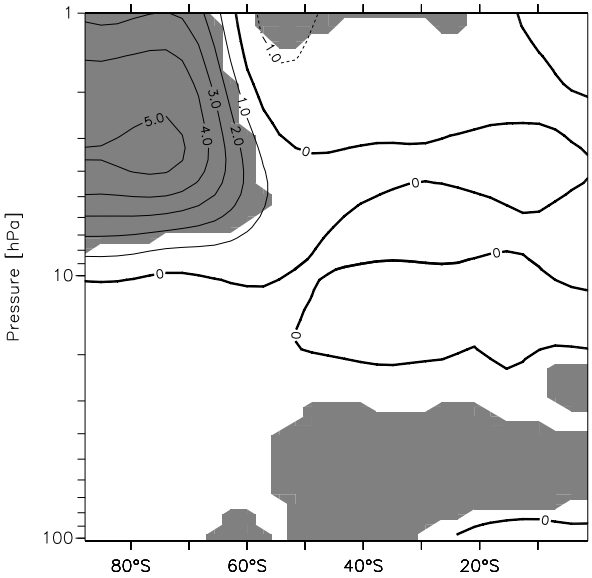

Fig. 7. Effects of the B-D circulation change on NO_x (contours, change in nmol/mol) during Southern Hemisphere winter and spring. The shaded area indicates statistical significance at the 1% level.

ACPD
10, 9895–9916, 2010

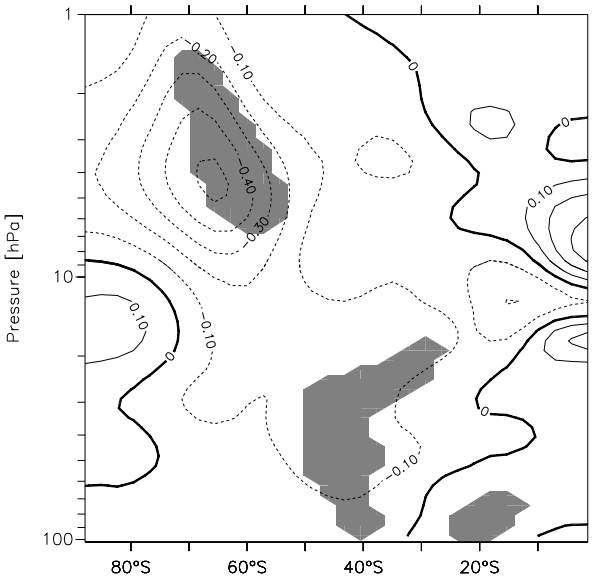

Fig. 8. Effects of the B-D circulation change on EEP NO_x induced ozone loss (contours, change in µmol/mol) during Southern Hemisphere winter and spring. The shaded area indicates statistical significance at the 5% level.

ACPD
10, 9895–9916, 2010